Microstructure, hardness and fracture resistance of P235TR1 seam steel pipes of different diameters

Walid Musrati[1], Bojan Međo[2], Ivana Cvijović-Alagić[3], Nenad Gubeljak[4], Primož Štefane[4], Zoran Radosavljević[5] and Marko Rakin[2]

[1]*University of El Mergib, Faculty of Engineering, Khoms, Libya*
[2]*University of Belgrade, Faculty of Technology and Metallurgy, Belgrade, Serbia*
[3]*University of Belgrade, Institute of Nuclear Sciences "Vinča", Belgrade, Serbia*
[4]*University of Maribor, Faculty of Mechanical Engineering, Maribor, Slovenia*
[5]*Research and Development Institute Lola, Belgrade, Serbia*

Abstract

Steel pipelines in industrial plants consist of different elements, including seamless and/or welded (seam) pipes. Properties of welded pipes, including their fracture behaviour, depend on the characteristics of both, the base metal, and the weld metal. In this work, two seam pipes are considered having different diameters and manufactured of P235TR1 steel. Hardness and microstructure were examined on the samples which contained the seam zone, to capture the influence of heterogeneity. Fracture resistance of the pipeline material, *i.e.* of both base metals and both seams, was determined by experimental examination of the recently proposed Pipe ring notch bending specimens with sharp stress concentrators. Differences between the two tested pipes, including the influence of the heterogeneity caused by the welded joint, were determined by comparison of the crack growth resistance curves. Effects of the initial stress concentrator shape, sharp machined notch or fatigue pre-crack are discussed.

Keywords: pipe ring testing; microstructural analysis; welded joint hardness; fracture mechanics; non-standard specimens.

Available on-line at the Journal web address: http://www.ache.org.rs/HI/

ORIGINAL SCIENTIFIC PAPER

UDC: 621.643.2-034.14: 620.163.4

Hem. Ind. **77(2)** 155-165 (2023)

1. INTRODUCTION

Pipelines in process industry plants can contain different types of sharp and/or blunt defects. Regardless of the moment when these defects occur, or their mechanism of initiation/development, they represent a risk that can endanger safe exploitation of the pipeline and the connected equipment. Therefore, the load carrying capacity, integrity, and failure resistance of pipes, as well as other process equipment elements (vessels [1,2], nozzles [3], valves [4], *etc.*), were considered in numerous studies, some of which will be mentioned in this section.

Generally, an important source of initial defects in pipelines are welds, which can be formed during fabrication (axial or spiral welds on seam pipes) or assembly (circumferential - girth joints). Examples of works which deal with the seam pipes are papers [5-7]. Quality testing for the pipes fabricated by different welding techniques is considered in [5], while fracture resistance comparison between the weld zones is presented in [6,7]. Mechanical properties and microstructure of the seam steel pipes were examined in literature [8], with a consideration of on-line spray water cooling (OSWC) process applied during manufacturing of the welded pipes. Besides longitudinally welded pipes, spiral welded pipes typically having larger diameters are also used in some applications. In a study on this type of pipes [9] influences of material anisotropy and spiral welding were analysed on the pipe behaviour under the loading.

Standards for the fracture toughness measurement typically require thick specimens, *i.e.* the requirement for the plane strain state is imposed. Two most frequently used standard specimens are SENB (Single Edge Notch Bending) and CT (Compact Tension) specimens. Such specimens for testing the pipeline material fracture resistance can be fabricated

Corresponding author: Bojan Međo, University of Belgrade, Faculty of Technology and Metallurgy, Belgrade, Serbia
E-mail: bmedjo@tmf.bg.ac.rs; Tel. +381 11 3370 505
Paper received: 23 February 2023; Paper accepted: 19 June 2023; Paper published: xx June 2023.
https://doi.org/10.2298/HEMIND230222016M

by cutting the pipes only if the pipe wall is relatively thick. To fabricate the required specimen geometries for thin-walled pipes, predominantly used in most industrial applications, is very problematic.

One of the alternative specimen geometries is proposed in literature [10]; termed the curved CT specimen. Their intention is to obtain the stress and stress distribution, which resemble those in a pressurised pipe with the initial defect in axial direction. However, the testing procedure requires fabrication of the appropriate rig which corresponds to only one pipe diameter.

Single edge notched tension (SENT) specimen type is applied by many authors in fracture analysis of pipes with circumferential position of the initial defect, including those positioned in the girth welded joints of the pipes. Comparison of SENT and SENB specimens, which have the same shape but different loading conditions, is shown in literature [11-13]. These studies revealed that SENB specimens give conservative results in some cases, and that SENT specimens are more appropriate for examination of pipes with circumferential cracks exposed to axial loading. As a result of the efforts of the researchers worldwide, SENT specimen geometry has been standardised in several countries. Unfortunately, it is not convenient for failure assessment of pipes exposed dominantly to internal pressures, where the most critical defects are positioned axially (*i.e.* critical stress is the hoop stress).

In several studies, tensile compact pipe (CP) specimens were proposed and examined [14,15]. This specimen consists of a pipe segment with a circumferential initial defect and two levers welded to its sides. The role of the levers is to transfer the loading from the testing machine.

A series of interesting thin-walled non-standard geometries were also proposed [16,17], where loading conditions and additional tools resemble the standard specimens. They are fabricated by cutting and subsequent shaping of the pipe segments and include both axial and circumferential positions of the pre-cracks.

A new specimen geometry (curved SENB) was also proposed [7] and it was compared with the standard CT specimen. This study was performed on seam API 5L X52 steel pipes. Cutting of the standard CT specimens was possible because the considered pipe had relatively thick walls. The work also included investigation of the seam fracture behaviour, as well as the difference between C-R and C-L directions (C-circumferential, R-radial, L-longitudinal).

Generally, all mentioned studies aimed at providing new possibilities for fracture examination of pipeline materials. They were performed on different pipeline steels, since many different materials are used in the process industry, depending on exploitation conditions of a particular plant/pipeline. The significance of material selection for pipelines is discussed in [18].

In this work, pipeline materials of two seam steel pipes were assessed by application of the recently proposed PRNB (Pipe ring notch bending) specimens [19], which have been experimentally and numerically examined and established previously [20-23]. The influence of residual stresses was also considered [24], while micromechanical analysis was the topic of a previous study [25]. The initial experimental results obtained on the larger-diameter pipes considered here were shown previously in [26] but were limited only to the pipe fracture behaviour. Here, microstructural analysis and hardness for both pipes are considered, and their fracture resistances are compared and discussed.

2. MATERIALS AND METHODS

Two groups of samples (for hardness and microstructural analysis) and specimens (for fracture examination) were prepared from seam pipes of two different diameters (Arcelor Mittal, Romania; the pipes were new, *i.e.* not previously used). The material of both pipes is P235TR1 steel, in accordance with the EN 10217-1 standard [27]. Chemical composition and tensile properties, obtained from the manufacturer certificate, are shown in Table 1, along with the standard requirements. In the Table, $R_{p0.2}$ is the conventional (proof) strength, R_m is the ultimate tensile strength and A is the elongation at fracture. Despite some deviations, properties of both pipe materials are within the bounds set by the standard for this material grade.

The samples for microstructural characterization and hardness testing were prepared by the standard metallographic technique, *i.e.* grind with SiC abrasive papers, polished by using diamond suspension, and cleaned in an ultrasonic bath with ethanol. The metallographically prepared samples were next subjected to etching with the Nital

reagent, containing 100 cm^3 of 96% ethanol and 3 cm^3 of 65 % nitric acid, for 30 s. The microstructural characteristics of both pipe materials were examined by optical microscopy (OM, Carl Zeiss Opton Axioplan, Carl Zeiss AG, Germany).

Table 1. Chemical composition and tensile properties of steel P235TR1 ($R_{p0.2}$ is the conventional (proof) strength, R_m is the ultimate tensile strength and A is the elongation at fracture) [27,28]

	Content, %						$R_{p0.2}$ / MPa	R_m / MPa	A / %
	C	Mn	S	P	Si	Al			
P235TR1 standard requirements	max 0.16	max 1.2	max. 0.02	max 0.025	max. 0.35	-	min. 235	360-500	min. 25
pipe ext. diam. 88.9 mm	0.08	0.52	0.013	0.014	0.02	0.043	389	417	40.2
pipe ext. diam. 168.3 mm	0.13	0.54	0.012	0.01	0.02	0.052	328	420	38

Figure 1 shows the samples used for hardness measurement; welded joint zone is included in examination. Hardness is measured by using a Buehler microindentation hardness tester (model Micromet 5101, Buehler, Germany) by applying a load of 1000 gf (9807 mN) for 15 s at positions along the measurement lines shown on each sample, while the seam width is determined by the microstructural analysis. The samples are denoted with respect to the pipe diameter: samples S168 (Figure 4a) and S89 (Figure 4b) for diameters 168.3 and 88.9 mm, respectively.

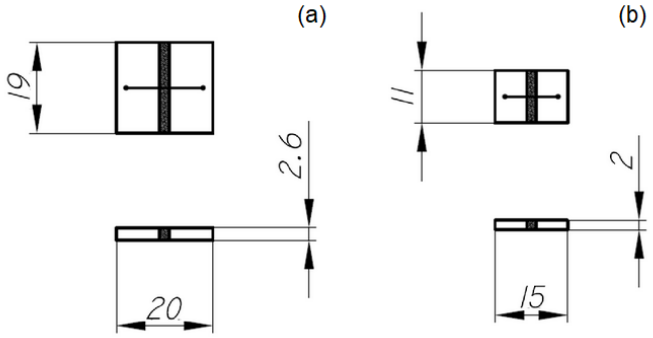

Figure 1. Samples for hardness measurement: (a) S168 and (b)S89

Fracture resistance, *i.e.* resistance to crack growth by ductile mechanism, is tested on recently proposed pipe ring notch bending specimens - PRNB. These specimens, as mentioned previously, have been developed as a convenient and reliable way for fracture testing of pipeline materials, especially thin-walled ones. The main specimen dimensions: external diameter *D*, width *W*, wall thickness *B* and sharp stress concentrator length a_0, are shown in Figure 2 and Table 2.

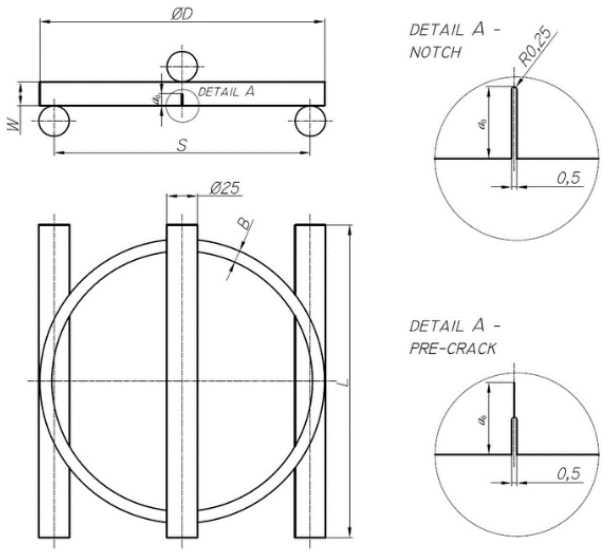

Figure 2. Specimen dimensions and testing scheme (Reprinted with permission from [23], Copyright by Elsevier, 2023

Machined notches were fabricated as stress concentrators on most specimens and fatigue pre-cracks were formed on a smaller-diameter specimen. The notches were formed by electrical discharge machining (EDM, Robofil 400, Charmilles, Switzerland), with the radius of 0.25 mm. Distance between the supports *S* is equal to 90 % of the external diameter for all specimens.

Table 2.Measures of pipe ring specimens: D -external diameter, W - width, B - wall thickness and a_0 - sharp stress concentrator length

	Position of the stress concentrators	*D* / mm	*B* / mm	*W* / mm	*W*/*B*	a_0/W
S-WM(168)-1	in WM and BM	168.18	3.21	12.99	≈ 4	0.5
S-WM(168)-2	in WM and BM	168.43	3.46	21.05	≈ 6	0.5
S-WM(168)-3	in WM and BM	168.21	3.24	19.26	≈ 6	0.5
S-BM(168)-6	in BM	168.28	3.22	19.23	≈ 6	0.5
S-WM(89)-7	in WM and BM	88.28	2.71	11.05	≈ 4	0.5
S-WM(89)-8	in WM and BM	88.59	2.58	10.48	≈ 4	0.5
S-BM(89)-9	in BM	88.62	2.55	10.30	≈ 4	0.45
S-BM(89)-10C	in BM - pre cracks	88.46	2.63	10.48	≈ 4	0.25 + crack = 0.38/0.46

Note: WM and BM stand for the weld metal (seam) and base metal, respectively

Digital image correlation (DIC) system Gom Aramis (Gom Metrology, Germany) [4,29,30] is applied for tracking the parameters related to deformation during the testing on the universal testing machine (model 1255, Instron, USA): displacement field, strain field, as well as CMOD - Crack mouth opening displacement and CTOD - Crack tip opening displacement. Aramis system consists of two cameras, acquisition equipment and software.

After the fracture testing, plastically deformed ring specimens are broken, after cooling in liquid nitrogen; this resulted in a brittle final fracture. Prior to this, the specimens were exposed to heating (in a furnace, during 30 min) to 400 °C, which enables a clear final crack distinction; this procedure is often called heat-tinting. Examination of fracture surfaces is performed on a stereo microscope (model SZX12, Olympus, Japan).

3. RESULTS AND DISCUSSION

3. 1. Hardness and microstructure

Microstructural analysis is performed by optical microscopy of etched welded joint (seam) samples. Figures 3-5 (sample S168) are obtained for the larger-diameter pipe, while the other microphotographs are obtained on the smaller-diameter pipe (Figures 6-8, sample S89) [31].

Two microconstituents are observed in the base metal (BM), shown in Figures 3a and 6a for both specimens: ferrite and pearlite. The former can be distinguished as white grains in these figures, while the latter is visible as dark islands positioned at the ferrite grain boundaries.

Figures 3b and 6b correspond to the weld metal (WM) of both pipes, and they are shown alongside each base metal. Ferrite can be seen as side plates nucleated at the austenite grain boundaries; additionally, fine acicular ferrite and ferrite-carbide aggregates (pearlite) are found. In the weld metal of the lower-diameter pipe (Figure 6b - sample S89), primary intragranular polygonal ferrite is also noticed.

Figures 4 and 5 contain transitions between the welded joint zones for the sample S168. In Figure 4, the transition base metal - heat affected zone (HAZ) is shown and the boundary is marked. Figure 4b represents a magnified part of Figure 4a marked by the rectangle. Inspection of the microstructure of this part of the transition zone reveals similar structures of the base metal and the heat affected zone. Microstructure in HAZ similar to the WM structure is observed only close to the fusion line, Figure 5.

Analysis of the variation of microstructure enabled estimation of the heat affected zone width: ~0.35 mm for sample S168 and cca. 0.4 mm for sample S89. In a similar way, overall variation of microstructure along the entire joint gives approximate weld metal widths: 2.6 mm for sample S168 and 2 mm for sample S89.

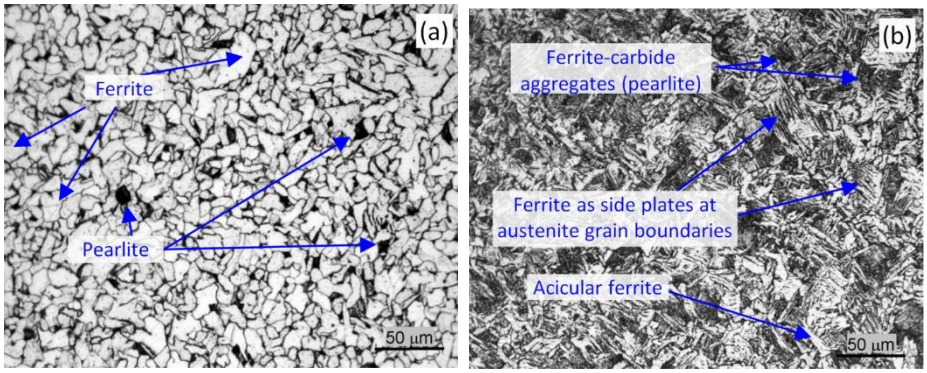

Figure 3. Micrographs of sample S168: (a) base metal and (b) weld metal

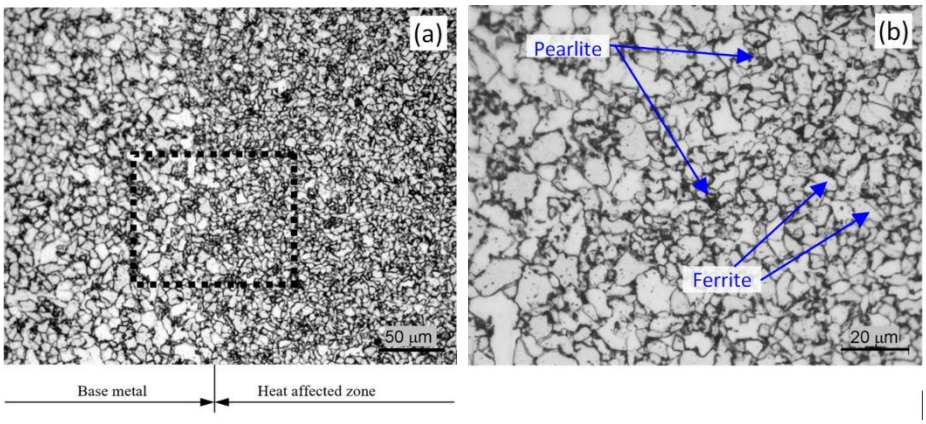

Figure 4. Micrographs of sample S168: (a) transition base metal - heat affected zone; (b) rectangular zone marked in (a) at higher magnification

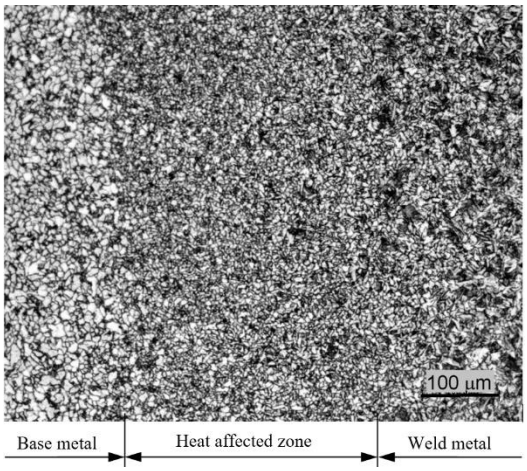

Figure 5. Micrograph of sample S168: Transition base metal - heat affected zone - weld metal

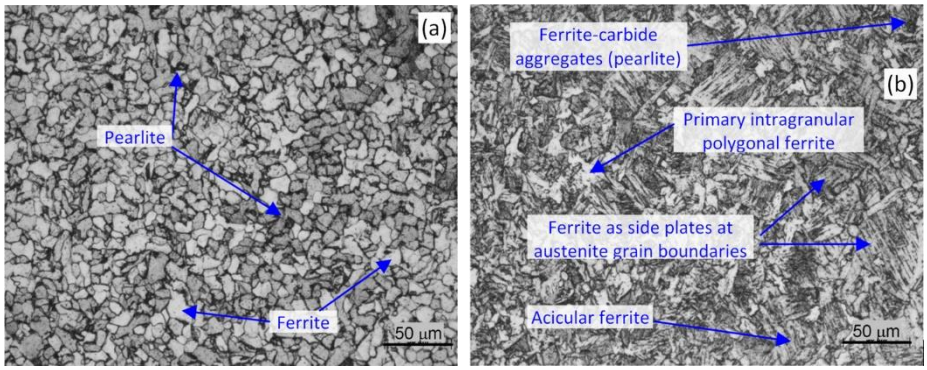

Figure 6. Micrographs of sample S89: (a) base metal and (b) weld metal

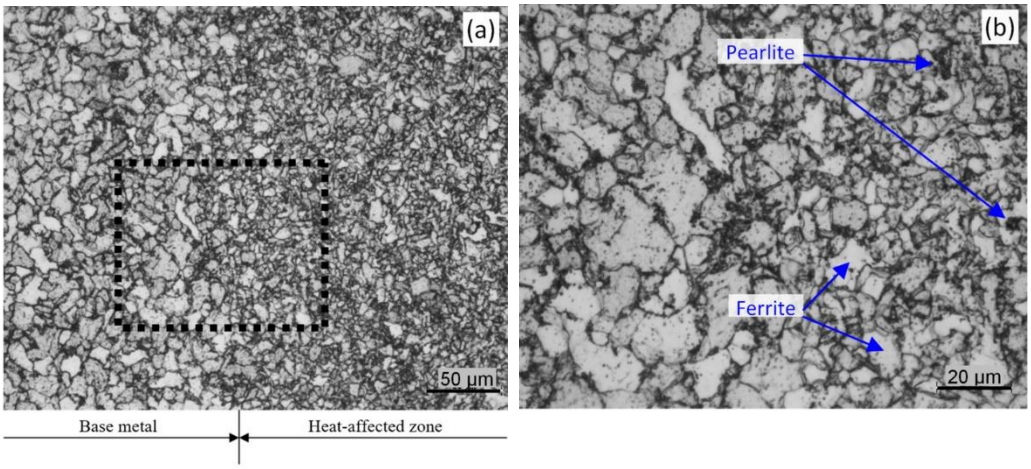

Figure 7. Micrographs of sample S89: (a) transition base metal - heat affected zone; (b) rectangular zone marked in (a) at higher magnification

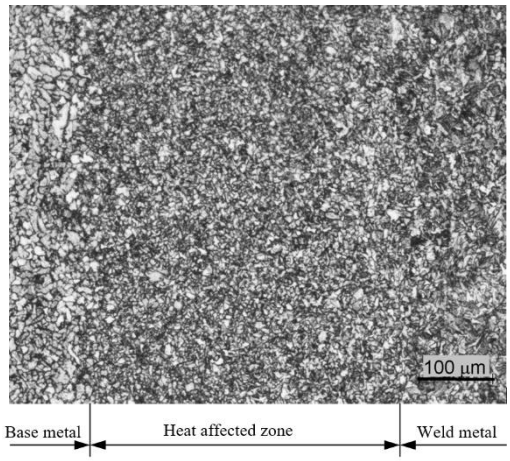

Figure 8. Micrograph of sample S89: Transition base metal - heat affected zone - weld metal

Variation in hardness across the seam region is presented in Figure 9. In these diagrams, the position and width of WM and HAZ, determined from the microphotographs, are also marked for both samples. Since the obtained values are higher in the seam zone, this hardness profile indicates overmatching.

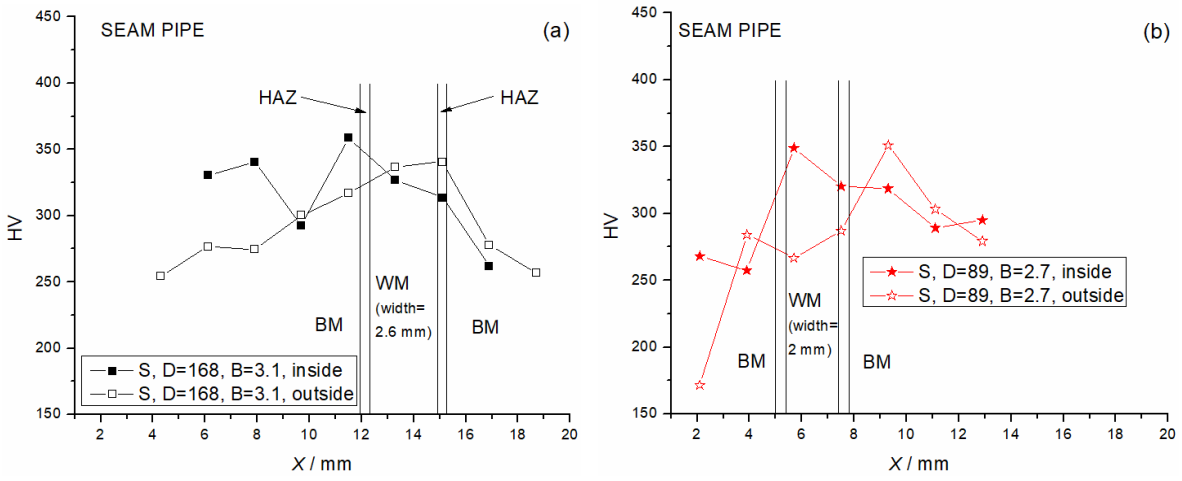

Figure 9. Variations in hardness across the joint - (a) sample S168 and (b)sample S89

Hardness is generally affected by the composition and ratio of phases present in the microstructure. Accordingly, the ratio of pearlite and ferrite in the microstructure shows a decisive influence on the hardness level of every single

region. Since pearlite is characterized by higher carbide content as compared to ferrite, the seam regions with higher contents of this phase are characterized by higher hardness. On the other hand, regions with more ferrite in the microstructure show lower hardness. In the analysed seams, a somewhat larger amount of pearlite is observed in the weld metal than in the base metal which corresponds to the higher hardness of this region. An increase in hardness in the heat affected zone and the base metal close to this zone was also observed.

3. 2. Fracture resistance examination

The final observed crack shape (Fig. 10) is characteristic for ductile fracture, *i.e.* growth of the crack is the most pronounced in the central part, due to the high stress triaxiality (*i.e.* much higher than in the vicinity of the specimen surfaces). This is obtained for both machined notches (Figs 10a,b), and fatigue pre-crack (Fig. 10c).

However, fatigue pre-cracking results in an uneven initial crack. This is caused by the cylindrical specimen shape, and fatigue crack growth is more pronounced on the internal side of the specimen (right-hand side of Figure 10c) than on the external one. However, even though the initial pre-crack is uneven, ductile crack growth is still relatively uniform, *i.e.* the crack length is the largest near the mid-thickness of the specimen.

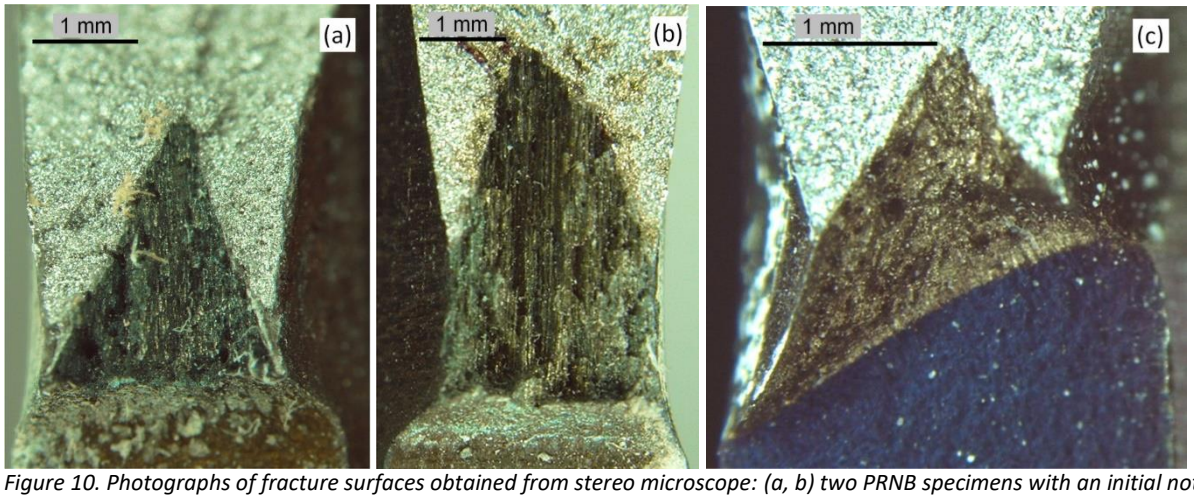

Figure 10. Photographs of fracture surfaces obtained from stereo microscope: (a, b) two PRNB specimens with an initial notch and (c)one with an initial fatigue pre-crack

As it was discussed and concluded previously [20], machined notch is a suitable stress concentrator for this geometry, and it gives reliable and repeatable results. As mentioned previously and shown in Figure 10, symmetric blunting and crack growth are obtained on the notched specimens. Also, it is possible to obtain a more precise and straight stress concentrator shape than for the fatigue pre-cracked specimens.

Figure 11 presents *F*-CMOD curves for the examined specimens (Fig. 11a for diameter 168.3 mm and Fig. 11b for diameter 88.9 mm); the force is obtained from the testing machine, while CMOD values are determined by the DIC system.

In these diagrams, basic measures of the specimens are shown alongside the specimen labels: the position of the stress concentrator, external diameter × wall thickness, ratio a_0/W, ratio W/B. For example, notation “Seam, 168.3x3.2, a0.5, W4” means that the specimen has one of the notches in the seam, diameter 168.3 mm, wall thickness B = 3.2 mm, ratio a_0/W = 0.5 and ratio W/B = 4 [31]. Near the legend, the stress concentrator position (WM or BM) is shown in all diagrams. The specimen 10C contains fatigue pre-cracks (therefore, letter C is included in its denotation), while the other ones contain machined notches.

The *F*-CMOD curves can be used to compare the load carrying capacity of structures with similar geometries. For example, in Figure 11a specimen 1 has significantly lower force values because its width-to-thickness ratio is 4, while for the remaining three specimens this value is 6. Also, there are some differences in the shape of these curves for the base and weld metal, if specimen 6 (BM) is compared with the specimens 2 or 3 (WM). However, these curves do not describe the development of fracture through the material, *i.e.* they do not include the crack growth data.

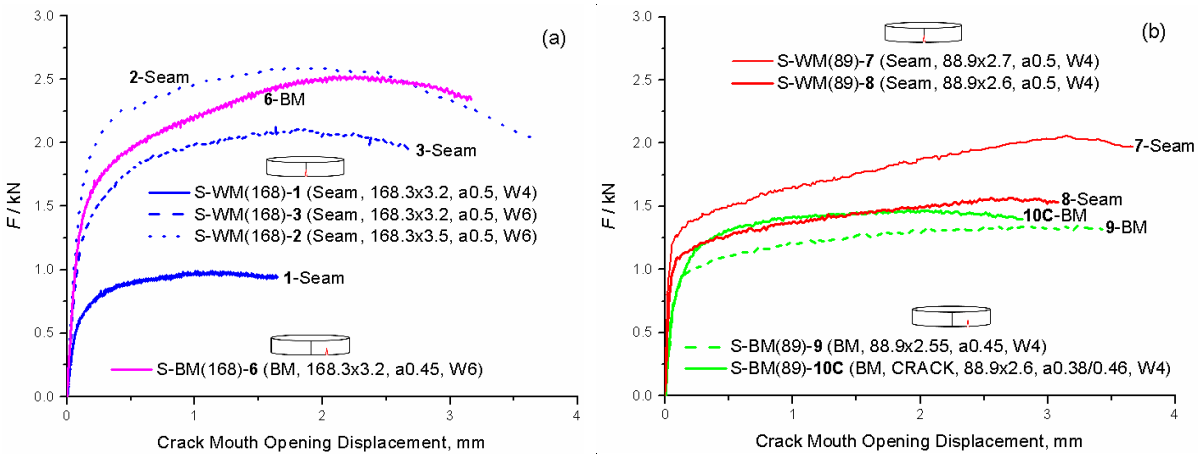

Figure 11. F-CMOD curves: ring specimens with D = 168.3 mm (a) and D = 88.9 mm (b); basic measures of the specimens with the specimen labels: e.g. "Seam, 168.3x3.2, a0.5, W4" means that the specimen has one of the notches in the seam, diameter 168.3 mm, wall thickness B = 3.2 mm, ratio a_0/W = 0.5 and ratio W/B = 4; the specimen 10C contains fatigue pre-cracks, while the other contain machined notches

The crack growth through all specimens is determined by the normalisation method [32], and these values are used in forming CTOD-Δ*a* curves, *i.e.* the crack growth resistance curves. In order to apply the normalisation method, the final crack length is measured on fracture surfaces; three of such surfaces are presented in Figure 10. In the following diagrams, δ_5 technique was used for measurement of CTOD, in accordance with the literature [33]. Therefore, denotation (CTOD-δ_5) is used and it is obtained by measurement by using the Aramis system, as the increase in the distance of two points, which are initially 5 mm apart (2.5 mm on each side of the initial tip of the stress concentrator).

CTOD-Δ*a* curves for both pipe base metals are shown in Figure 12; this diagram reveals two important trends. First, the smaller pipe is significantly more resistant to crack growth than the larger pipe. Also, the result obtained for the fatigue pre-cracked specimen S-BM(89)10C is very similar to that obtained for the specimen with notches S-BM(89)9.

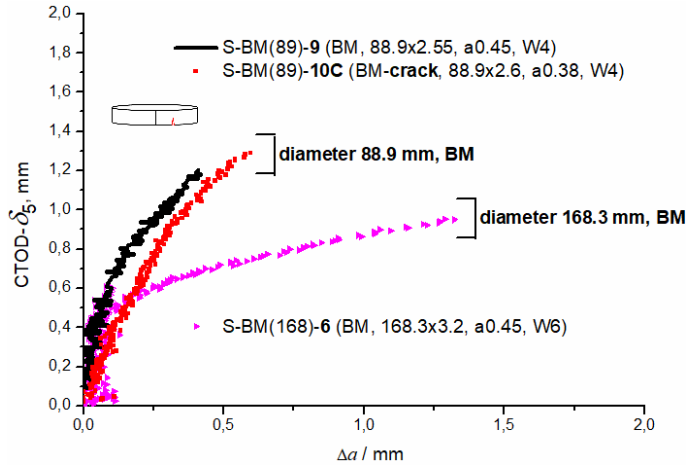

Figure 12. CTOD-Δa curves of the base metal for the two pipe diameters

In Figure 13, crack growth resistance curves for weld metals (seams) for both pipe diameters are shown. Similarly as for the base metals, the seam of the smaller-diameter pipe exhibits higher fracture resistance.

Finally, in order to have an overall view of the fracture testing results, all 4 materials are shown in Figure 14, *i.e.* both base metals and both weld metals (seams). Higher resistance to crack growth of the lower-diameter pipe is mentioned above. However, there is also another significant difference: the base metal and the seam in the smaller diameter pipe show more similar fracture behaviours than those in the larger diameter pipe.

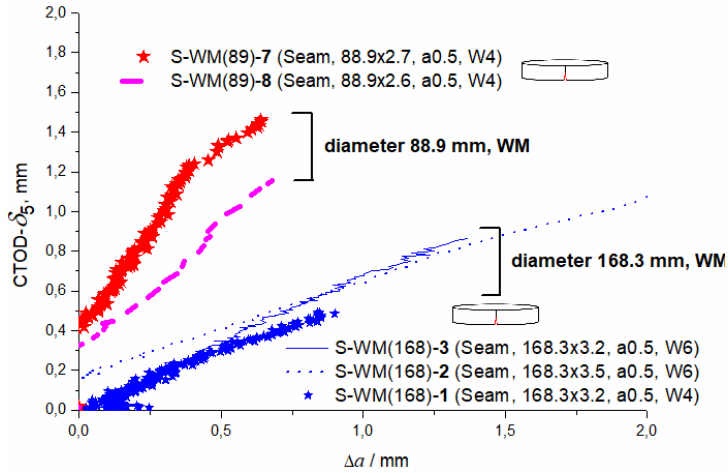

Figure 13. CTOD-Δa curves of the seam for the two pipe diameters

Generally, the results show a pronounced dependence of fracture resistance on material properties, rather than on the specimen or stress concentrator dimensions, which is certainly favourable.

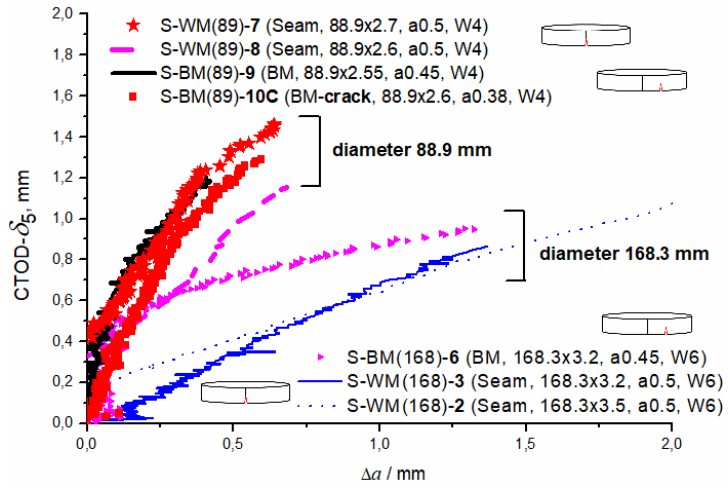

Figure 14. CTOD-Δa curves of the base metal and seam for the two pipe diameters

4. CONCLUSION

This work presents examination of hardness, microstructure and fracture toughness of two seam pipes fabricated of the same material, but with different diameters. Despite the similarity of the materials, hardness and microstructure, the base metals exhibit significantly different fracture resistances, expressed by the crack growth resistance curves. Also, another difference is determined: while the larger-diameter pipe base metal is more resistant to fracture than its weld metal, the smaller-diameter pipe exhibits different behaviour – the base and weld metals are characterised by similar fracture resistances. It can be said that testing of the pipe ring specimens successfully captured these differences between the examined pipes. The influence of the stress concentrator shape is also assessed on one of the smaller-diameter ring specimens, and an EDM notch resulted in similar fracture resistance as a fatigue pre-crack for this material. Having in mind that the vast majority of pipelines in process industry consist of thin-walled pipes, the new specimen geometry has a good potential for application in material selection, fracture testing, integrity assessment and safety assurance procedures.

Acknowledgements**:** *This work was supported by the Ministry of Science, Technological Development and Innovation of the Republic of Serbia (Contract No. 451-03-47/2023-01/200135).*

REFERENCES

[1] Moattari M, Moshayedi H, Sattari-Far I. Application of new constraint based Master Curve in fracture assessment of pressure vessels. *Int J Pres Ves Pip*. 2019; 174: 25–31. https://doi.org/10.1016/j.ijpvp.2019.05.009

[2] Golubović T, Sedmak A, Spasojević Brkić V, Kirin S, Veg E. Welded joints as critical regions in pressure vessels - case study of vinyl chloride monomer storage tank. *Hem Ind*. 2018; 72: 177–182. https://doi.org/10.2298/HEMIND171009006G

[3] Murtaza UT, Javed Hyder M. Fracture analysis of the set-in nozzle of a PWR reactor pressure vessel - Part 1: Determination of critical crack. *Eng Fract Mech*. 2018; 192: 343–361. https://doi.org/10.1016/j.engfracmech.2016.03.049

[4] Mitrović N, Petrović A, Milošević M, Momčilović N, Mišković Ž, Maneski T, Popović P. Experimental and numerical study of globe valve housing. *Hem Ind*. 2017; 71: 251–257. https://doi.org/10.2298/HEMIND160516035M

[5] Šarkoćević Ž, Rakin M, Arsić M, Sedmak A. Fabrication of high strength seam welded steel tubes and quality indicator testing. *Struct Integr Life*. 2008; 8: 81–98. http://divk.inovacionicentar.rs/ivk/ivk08/ivk0802-1.html

[6] Choupani N, Asghari V, Kurtaran, H. Fracture Characterization of Base Metal, Seam Weld, and Girth Weld of Welded Line Pipe Steel at Room and Low Temperatures. *J Mater Eng Perf*. 2021; 30: 1046–1053. https://dx.doi.org/10.1007/s11665-020-05431-3

[7] Angeles-Herrera D, Albiter-Hernández A, Cuamatzi-Meléndez R, González-Velázquez JL. Fracture toughness in the circumferential-longitudinal and circumferential-radial directions of longitudinal weld API 5L X52 pipeline using standard C(T) and nonstandard curved SE(B) specimens. *Int J Fract*. 2014; 188: 251–256. https://dx.doi.org/10.1007/s10704-014-9949-1

[8] Chen Z, Chen X, Zhou T. Microstructure and Mechanical Properties of J55ERW Steel Pipe Processed by On-Line Spray Water Cooling. *Metals*. 2017; 7: paper No. 150. https://doi.org/10.3390/met7040150

[9] Van Minnebruggen K, Hertelé S, Thibaux P, De Waele W. Effects of specimen geometry and anisotropic material response on the tensile strain capacity of flawed spiral welded pipes. *Eng Fract Mech*. 2015; 148: 350–362. https://doi.org/10.1016/j.engfracmech.2015.04.031

[10] Gajdos L, Sperl M. Evaluating the integrity of pressure pipelines by fracture mechanics. In: *Applied Fracture Mechanics*, London: InTech Publishing; 2012: 283–310. https://dx.doi.org/10.5772/51804

[11] Zhang ZL, Xu J, Nyhus B, Østby E. SENT (single edge notch tension) methodology for pipeline applications. *In: Proceedings of the 18th European Conference on Fracture*, Dresden, Germany, 2010, pp. 1-8, published on CD.

[12] Xu J, Zhang ZL, Østby E, Nyhus B, Sun DB. Effects of crack depth and specimen size on ductile crack growth of SENT and SENB specimens for fracture mechanics evaluation of pipeline steels. *Int J Pres Ves Pip*. 2009; 86: 787–797. https://dx.doi.org/10.1016/j.ijpvp.2009.12.004

[13] Xu J, Zhang ZL, Østby E, Nyhus B, Sun DB. Constraint effect on the ductile crack growth resistance of circumferentially cracked pipes. *Eng Fract Mech*. 2010; 77: 671–684. https://dx.doi.org/10.1016/j.engfracmech.2009.11.005

[14] Mahajan G, Saxena S, Mohanty A. Numerical characterization of compact pipe specimen for stretch zone width assessment. *Fatigue Fract Engng Mater Struct*. 2016; 39: 859–865. https://dx.doi.org/10.1111/ffe.12400

[15] Koo JM, Park S, Seok CS. Evaluation of fracture toughness of nuclear piping using real pipe and tensile compact pipe specimens. *Nucl Eng Design*. 2013; 259: 198–204. https://dx.doi.org/10.1016/j.nucengdes.2013.03.001

[16] Bergant M, Yawny A, Perez Ipiña J. Experimental determination of J-resistance curves of nuclear steam generator tubes. *Eng Fract Mech*. 2016; 164: 1–18. https://dx.doi.org/10.1016/j.engfracmech.2016.07.008

[17] Bergant M, Yawny A, Perez Ipiña J. Numerical study of the applicability of the g-factor method to J-resistance curve determination of steam generator tubes using non-standard specimens. *Eng Fract Mech*. 2015; 146: 109–120. https://dx.doi.org/10.1016/j.engfracmech.2015.07.059

[18] Capelle J, Pluvinage G, Modification of failure risk by the use of high strength steels in pipelines, *Struct Integr Life*. 2013: 13; 23–27 http://divk.inovacionicentar.rs/ivk/ivk13/ivk1301-4.html

[19] Matvienko YG, Gubeljak N. Model for Determination of crack-resistance of the pipes. Patent No. RU 2564696 C, 2015 (in Russian)

[20] Gubeljak N, Likeb A, Matvienko Y. Fracture toughness measurement by using pipe-ring specimens. *Proc Mater Sci*. 2014; 3: 1934–1940. https://dx.doi.org/10.1016/j.mspro.2014.06.312

[21] Likeb A. Suitability of pipe-ring specimen for determination of fracture toughness. PhD Thesis, University of Maribor, Faculty of Mechanical Engineering, Slovenia, 2014 (in Slovenian)

[22] Likeb A, Gubeljak N, Matvienko Y. Finite element estimation of the plastic ηpl factors for pipe-ring notched bend specimen using the load separation method. *Fatigue Fract Eng Mater Struct*. 2014; 37: 1319–1329. https://dx.doi.org/10.1111/ffe.12173

[23] Musraty W, Medjo B, Gubeljak N, Likeb A, Cvijović-Alagić I, Sedmak A, Rakin M. Ductile fracture of pipe-ring notched bend specimens - micromechanical analysis. *Eng Fract Mech*. 2017; 175: 247–261. https://dx.doi.org/10.1016/j.engfracmech.2017.01.022

[24] Damjanović D, Kozak D, Gubeljak N. The influence of residual stresses on fracture behavior of Pipe Ring Notched Bend specimen (PRNB), *Eng Fract Mech*. 2019; 205: 347–358. https://dx.doi.org/10.1016/j.engfracmech.2018.10.016

[25] Musrati W, Međo B, Gubeljak N, Štefane P, Veljić D, Sedmak A, Rakin M. Fracture assessment of seam and seamless steel pipes by application of the ring-shaped bending specimens. *Theor Appl Fract Mech*. 2019; 103: paper No. 102302. https://dx.doi.org/10.1016/j.tafmec.2019.102302

[26] Musraty W., Međo B., Gubeljak N., Štefane P., Radosavljević Z., Burzić Z., Rakin M. Seam pipes for process industry - fracture analysis by using ring-shaped specimens. *Hem Ind*. 2018; 72: 39–46. https://dx.doi.org/10.2298/HEMIND170530014M
[27] EN 10217-1: Welded steel tubes for pressure purposes. Technical delivery conditions Electric welded and submerged arc welded non-alloy steel tubes with specified room temperature properties, 2019.
[28] Inspection certificates No. 31042 and No. 33131/1, Arcelor Mittal Tubular Products Iasi S.A., Romania, 2015.
[29] GOM Precise Industrial 3D Metrology. www.gom.com. Accessed in January, 2023.
[30] Gubeljak N. Application of stereometric measurement on structural integrity. *Struct Integr Life*. 2006; 6: 65–74. http://divk.inovacionicentar.rs/ivk/ivk06/ivk0601-7.html
[31] Musrati W. Characterisation of damage and fracture of pipeline material using ring-shaped specimens. PhD Thesis, University of Belgrade, Faculty of Technology and Metallurgy, Serbia, 2019.
[32] ASTM E1820: Standard test method for measurement of fracture toughness. 2015.
[33] Displacement gauge system for applications in fracture mechanics. Patent Publication, GKSS Research Center, Geesthacht, Germany, 1991.

Otpornost prema lomu, tvrdoća i mikrostruktura šavnih cevi različitog prečnika izrađenih od čelika P235TR1

Walid Musrati[1], Bojan Međo[2], Ivana Cvijović-Alagić[3], Nenad Gubeljak[4], Primož Štefane[4], Zoran Radosavljević[5] i Marko Rakin[2]

[1]University of El Mergib, Faculty of Engineering, Khoms, Libya
[2]Univerzitet u Beogradu, Tehnološko-metalurški fakultet, Beograd, Srbija
[3]Univerzitet u Beogradu, Institut za nuklearne nauke "Vinča", Beograd, Srbija
[4]Univerzitet u Mariboru, Mašinski fakultet, Maribor, Slovenija
[5]Istraživačko-razvojni institut Lola, Beograd, Srbija

(Naučni rad)

Izvod

Čelični cevovodi u industrijskim postrojenjima se sastoje od različitih elemenata, uključujući bešavne i/ili zavarene (šavne) cevi. Osobine šavnih cevi, uključujući ponašanje materijala cevi pri lomu, zavise i od osnovnog metala i od metala šava. U ovom radu razmatrane su dve šavne cevi različitih prečnika, izrađene od čelika P235TR1. Tvrdoća i mikrostruktura su analizirane na uzorcima isečenim iz cevi u zoni šava, da bi se odredio uticaj heterogenosti. Otpornost prema lomu materijala cevovoda, tj. oba osnovna metala i oba šava, je određena na osnovu ispitivanja epruveta oblika prstena sa oštrim koncentratorima napona, predloženih u prethodnim studijama. Poređenjem krivih otpornosti prema rastu prsline određene su razlike između dve ispitivane cevi, kao i uticaj heterogenosti izazvan postojanjem zavarenog spoja. Razmotren je uticaj oblika početnog koncentratora napona, oštrog žleba odnosno zamorne početne prsline.

Ključne reči: ispitivanje epruveta oblika prstena; mikrostrukturna analiza; tvrdoća zavarenog spoja; mehanika loma; nestandardne epruvete